Article

Entropic Stabilization of Isolated β-Sheets

Philippe Dugourd, Rodolphe Antoine, Gary Breaux, Michel Broyer, and Martin F. Jarrold

J. Am. Chem. Soc., **2005**, 127 (13), 4675-4679• DOI: 10.1021/ja0437499 • Publication Date (Web): 12 March 2005

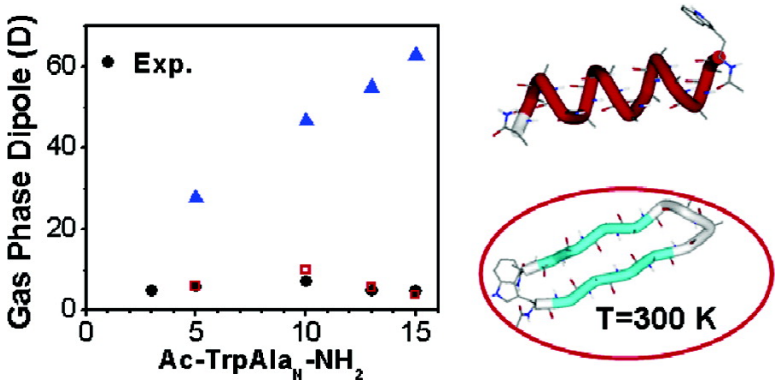

More About This Article

Additional resources and features associated with this article are available within the HTML version:

- Supporting Information
- Links to the 6 articles that cite this article, as of the time of this article download
- Access to high resolution figures
- Links to articles and content related to this article
- Copyright permission to reproduce figures and/or text from this article

View the Full Text HTML

J|A|C|S
ARTICLES
Published on Web 03/12/2005

Entropic Stabilization of Isolated β-Sheets

Philippe Dugourd,*,† Rodolphe Antoine,† Gary Breaux,‡ Michel Broyer,† and Martin F. Jarrold*,‡

Contribution from the Laboratoire de Spectrométrie Ionique et Moléculaire, UMR No. 5579, CNRS et Université Lyon 1, 43 bd du 11 novembre 1918, 69622 Villeurbanne Cedex, France, and Chemistry Department, Indiana University, 800 East Kirkwood Avenue, Bloomington, Indiana 47405-7102

Received October 14, 2004; E-mail: dugourd@lasim.univ-lyon1.fr; mfj@indiana.edu

Abstract: Temperature-dependent electric deflection measurements have been performed for a series of unsolvated alanine-based peptides (Ac-WA$_n$-NH$_2$, where Ac = acetyl, W = tryptophan, A = alanine, and n = 3, 5, 10, 13, and 15). The measurements are interpreted using Monte Carlo simulations performed with a parallel tempering algorithm. Despite alanine's high helix propensity in solution, the results suggest that unsolvated Ac-WA$_n$-NH$_2$ peptides with $n > 10$ adopt β-sheet conformations at room temperature. Previous studies have shown that protonated alanine-based peptides adopt helical or globular conformations in the gas phase, depending on the location of the charge. Thus, the charge more than anything else controls the structure.

Introduction

Understanding the factors that stabilize secondary structure elements (helices and sheets) is critical to understanding protein folding and relevant to conformational diseases such as Alzheimer's where soluble proteins are converted into insoluble quaternary structures with high β-sheet content.[1−3]Many aspects of the protein folding problem remain poorly understood because of the complex mixture of intermolecular and intramolecular interactions that are present.[4] Studies of simple model systems under well-characterized conditions help to identify the critical issues.[5,6] Here we report studies of the conformations of a series of neutral, unsolvated alanine-based peptides. While alanine is known to be a strong helix former in solution, our results suggest that the preferred room temperature conformation for isolated, neutral, alanine-based peptides is an antiparallel β-sheet.

To date, spectroscopy has provided most of what is known about the conformations of neutral, unsolvated biomolecules.[7,8] However, this approach is still limited to small systems such as isolated amino acids and small peptides. Here, we report measurements of the average electric dipole moments of unsolvated Ac-WA$_n$-NH$_2$ (Ac = acetyl, W = tryptophan, and A = alanine) peptides with n = 3, 5, 10, 13, and 15. By comparing the measured dipole moment to dipole moments calculated for model structures we deduce information about the conformation of the peptide. For example, α-helices have large dipole moments because the dipoles associated with the peptide bonds align to form a macro-dipole,[9] while β-sheets have small dipole moments because the dipoles associated with the peptide bonds almost cancel.

Experimental Methods

The measurements were performed on an apparatus consisting of a matrix-assisted laser-desorption (MALD) source coupled to a molecular beam deflection apparatus with a position-sensitive time-of-flight mass spectrometer.[10,11] Ac-WA$_n$-NH$_2$ peptides with n = 3, 5, 10, 13, and 15 were synthesized using FastMoc chemistry on an Applied Biosystems model 433A peptide synthesizer. After synthesis, they were cleaved from the HMP resin using a 95% TFA and 5% water v/v mixture, precipitated using cold diethyl ether, and lyophilized. MALD targets were prepared by pressing a 1:3 mass ratio of the unpurified peptide and high-purity cellulose powder. In the source, the peptides are desorbed with the third harmonic of a pulsed Nd:YAG laser (355 nm) and entrained in a pulsed helium flow generated with a piezoelectric valve. As the molecular beam leaves the source, the peptides are thermalized in a 5-cm long diverging nozzle. In some of the experiments the temperature of the nozzle was raised to heat the peptides. After exiting the nozzle, the beam is tightly collimated by two slits before it travels through the 15-cm long electric deflector. The deflector provides an electric field F and a field gradient ($\partial F/\partial z$) perpendicular to the beam axis. One meter after the deflector, the molecular beam is irradiated with the fourth harmonic of a Nd:YAG laser (266 nm) in the extraction region of the position-sensitive time-of-flight mass spectrometer. The two-photon ionization efficiency is enhanced because

† CNRS et Université Lyon 1.
‡ Indiana University.

(1) Dobson, C. M. *Nature* **2002**, *418*, 729−730.
(2) Ellis, R. J.; Pinheiro, T. J. T. *Nature* **2002**, *416*, 483−484.
(3) Koo, E. H.; Lansbury, P. T.; Kelly, J. W. *Proc. Natl. Acad. Sci. U.S.A.* **1999**, *96*, 9989−9990.
(4) Dill, K. A. *Biochemistry* **1990**, *29*, 7133−7155.
(5) Jarrold, M. F. *Annu. Rev. Phys. Chem.* **2000**, *51*, 179−207.
(6) Peng, Y.; Hansmann, U. H. E. *Phys. Rev. E* **2003**, *68*, 041911.
(7) Robertson, E. G.; Simons, J. P. *Phys. Chem. Chem. Phys.* **2001**, *3*, 1−18.
(8) Dian, B. C.; Longarte, A.; Mercier, S.; Evans, D. A.; Wales, D. J. Zwier, T. S. *J. Chem. Phys.* **2002**, *117*, 10688−10702.
(9) Hol, W. G. J.; Duijnen, P. T.; Berendsen, H. J. C. *Nature* **1978**, *273*, 443−446.
(10) Compagnon, I.; Hagemeister, F. C.; Antoine, R.; Rayane, D.; Broyer, M.; Dugourd, P.; Hudgins, R. R.; Jarrold, M. F. *J. Am. Chem. Soc.* **2001**, *123*, 8440−8441.
(11) Antoine, R.; Compagnon, I.; Rayane, D.; Broyer, M.; Dugourd, P.; Breaux, G.; Hagemeister, F. C.; Pippen, D.; Hudgins, R. R.; Jarrold, M. F. *J. Am. Chem. Soc.* **2002**, *124*, 6737−6741.

10.1021/ja0437499 CCC: $30.25

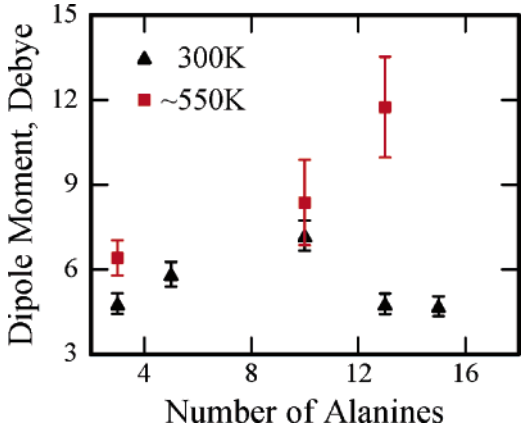

Figure 1. Plot of the measured dipole moments against peptide size. Measurements with the source nozzle extension at 300 K (filled triangle) and at ~550 K (filled red square) are shown.

the photon energy is near resonant for the indole moiety in tryptophan. The velocity of the peptides is selected and measured with a mechanical chopper synchronized with the ionization laser pulse.

Experimental Results

There are two limiting cases: for a rigid molecule the beam profile is symmetrically broadened in the deflector, while for a nonrigid molecule (i.e. where the vibrational and rotational Hamiltonians are not separable) the beam is globally deflected toward the high field.[10,11] For the peptides studied here, the beams are all uniformly deflected, indicating that the individual molecules in the beam have similar average dipole moments. The deflection was measured as a function of the field in the deflector, and shows the expected linear dependence on the square of the deflector voltage. The deflection is given by

$$d = \frac{K}{mv^2}\chi F\frac{\partial F}{\partial z} \tag{1}$$

where K is a geometrical factor, m is the mass of the peptide, v is the velocity, and χ is the electric susceptibility. Assuming a linear response, the electric susceptibility is related to the electric polarizability, α, and the average square dipole moment by the Langevin−Debye equation:[12]

$$\chi = \alpha + \frac{\langle \mu^2 \rangle_{T,F=0}}{3kT} \tag{2}$$

This expression is valid in the low-field/high-temperature limit. It assumes that there is a canonical distribution before the molecules enter the deflector and that the correlation of the dipole on the axis of the electric field tends toward zero as the molecules travel through the deflector, $\langle \mu_z(t=0)\mu_z(t)\rangle \rightarrow 0$ (i.e. a loss of memory of the orientation of the rotational motion). The polarizability is estimated from an additive model and subtracted from the susceptibility.[13] The average dipole moments determined in this way are plotted in Figure 1. The room temperature dipole moments (filled triangles) initially increase, peak at Ac-WA_{10}-NH_2, and then decrease. Dipole moments measured with the source nozzle heated to ~550 K are also shown in Figure 1 (as filled red squares). The high temperature dipoles appear to systematically increase with peptide size.

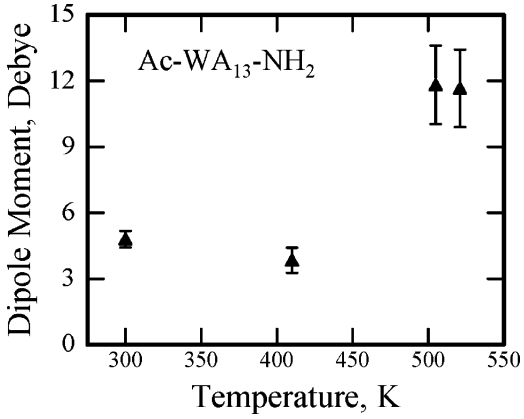

Figure 2. Plot of the dipole moments measured for Ac-WA_{13}-NH_2 as a function of the temperature of the source nozzle.

Dipole moments measured for Ac-WA_{13}-NH_2 as a function of temperature are shown in Figure 2. There appears to be a sharp increase in the dipole between 400 and 500 K.

Parallel Tempering Simulations. To help analyze the experimental results we have performed Monte Carlo (MC) simulations with a parallel tempering algorithm.[14] This algorithm allows one to explore the conformational landscape and to identify low free energy structures as a function of temperature. The Amber96 force field was used to provide potential energies for the conformations sampled in the simulations.[15] In parallel tempering, N parallel MC simulations are run at different temperatures, and transitions are permitted between neighboring temperatures. For Ac-WA_n-NH_2 with $n = 3$, 5, 10, 13, and 15, we used $N = 15$, 23, 31, 31, and 47 temperatures between 100 and 1250 K, respectively. The spacing between the temperatures is given by

$$T_i = 0.85\,T_{\max}\left(\frac{T_{\min}}{T_{\max}}\right)^{i/(N-1)} + 0.15\left(T_{\max} - \frac{i}{N-1}(T_{\max} - T_{\min})\right)\ (0 \le i \le N-1) \tag{3}$$

In each MC simulation, we randomly updated all atomic coordinates and dihedral angles in the backbone and in the tryptophan and lysine side chains. Exchanges between neighboring temperatures were attempted every 10 MC sweeps (a sweep consists of one move for each dihedral angle and 5M atomic moves where M is the number of atoms). Exchange between two replicas i and $j = i + 1$ are accepted with a probability given by

$$\rho = \min(1, \exp[-(\beta_i - \beta_j)(E_j - E_i)]) \tag{4}$$

where E_i is the potential energy and β_i is the reciprocal temperature of replica i ($\beta_i = 1/k_B T_i$ where T_i is the temperature and k_B is Boltzmann's constant). Two parallel tempering runs with $31-259 \times 10^6$ MC steps at each temperature were performed for each peptide. The total energy and the configuration of each residue (α, β, or other) were monitored at every MC step after a thermalization run of 22,000 sweeps. A residue is labeled α-helical if the backbone dihedral angles $\phi = -60$

(12) Debye, P. *Polar Molecules*; Dover Publications: New York, 1929.
(13) Miller, K. J. *J. Am. Chem. Soc.* **1990**, *112*, 8533−8542.
(14) Hansmann, U. H. E. *Chem. Phys. Lett.* **1997**, *281*, 140−150.
(15) Cornell, W. D.; Cieplak, P.; Bayly, C. I.; Gould, I. R.; Merz, K. M.; Ferguson, D. M.; Spellmeyer, D. C.; Fox, T.; Caldwell, J. W.; Kollman; P. A. *J. Am. Chem. Soc.* **1995**, *117*, 5179−5197.

$\pm$ 40° and $\psi = -46 \pm 40°$ and β-sheet if $\phi = -150 \pm 40°$ and $\psi = -150 \pm 40°$. Free energy maps were obtained through the weighted histogram analysis method.[16] The dipole moment for each conformation was computed using

$$\mu = \sum_i q_i r_i \qquad (5)$$

where q_i are the partial charges and r_i the positions of each atom according to the Amber96 parameter set. Comparisons with dipole moments calculated using density functional theory have shown this to be a good approximation. The random walk of each replica over all temperatures and the acceptance rate for exchange moves were monitored and used as convergence criteria. For $n = 3$ and 5 the parallel tempering algorithm provides good sampling of the energy landscape, but for the larger peptides the coverage is less thorough, the lowest-energy structures may not be found, and average quantities derived from the simulations will differ (at least by a small amount) from the true thermodynamic averages. For the larger peptides, organized structures tend to appear late in the simulations and so their statistical weights may be underestimated.

Four main types of conformations emerged from the simulations: α-helices, β-sheets, globules (compact random-looking three-dimensional structures), and random coils (unfolded structures found at high temperatures). For the β-sheets, U-shaped β-hairpins and S-shaped conformations with two β-turns coexist. In solution, alanine is known to have a high helix propensity,[17] but it also possesses the structural flexibility to form other structures[18−21] including alanine-rich β-sheet complexes. For Ac-WA_n-NH_2 with $n > 10$, the lowest potential energy conformations found in the simulations are α-helices. This is consistent with previous calculations on similar alanine-rich peptides.[19,22] However, at room temperature, the difference in potential energy is overcome by entropy, and the α-helix is not the lowest free energy structure.

Free energy maps obtained using the weighted histogram analysis method[16] for Ac-WA_{13}-NH_2 at $T = 100$ and 300 K are shown in Figure 3. The horizontal and vertical axes correspond to the number of residues in α-helical and β-sheet conformations, respectively. The colored contours show the free energy, and the lowest free energy regions are red. Representative conformations from the free energy minima at 100 and 300 K are shown at the bottom of Figure 3. At 100 K the lowest free energy conformations are α-helices. The free energy minimum at around $N_{\mathrm{Beta}} \approx 3$ and $N_{\mathrm{Alpha}} \approx 2$ corresponds to globules. At 300 K there is a broad minimum in the free energy at close to the origin (corresponding to globules) and a smaller minimum with $N_{\mathrm{Beta}} \approx 9$ (corresponding to β-sheets). Both β-hairpins (conformation b in Figure 3) and S-shaped β-sheets (c in Figure 3) contribute to the β-sheet region of the map, although the

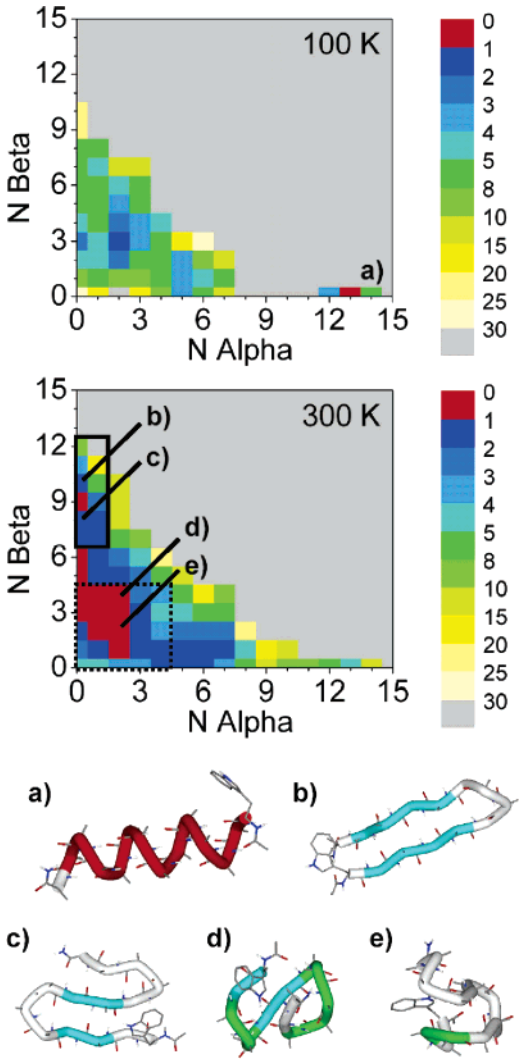

Figure 3. Free energy maps (G/kT) for Ac-WA_{13}-NH_2 at $T = 100$ and 300 K. The horizontal and vertical axes correspond to the number of residues in α-helical and β-sheet conformations, respectively. The colored contours show the free energy, the lowest free energy regions are colored in red. The boxes show the regions used to compute the average dipole values for β-sheet (full line) and globule (dashed line). (a) Representative helical conformation from the 100 K simulations. (b and c) Representative β-sheet conformations from the 300 K simulations. (d and e) Representative globule conformations from the 300 K simulations.

hairpins are more abundant at room temperature. The calculated statistical weights for the conformations encountered in the simulations may depend on the nature of the force field, as found in several recent studies.[23,24] However, in the present case we are able to compare the simulations with experimental results and gain some insight into the performance of the force field employed.

Discussion

Figure 4 shows a comparison of the measured and calculated dipole moments. Canonical ensemble average dipole moments obtained by averaging over the entire free energy map are plotted as blue stars in the lower half of the figure. For Ac-WA_n-NH_2 with $n = 3$ and 5 the calculated average dipoles are in excellent

(16) Kumar, S.; Bouzida, D.; Swendsen, R. H.; Kollman, P. A.; Rosenberg, J. M. *J. Comput. Chem.* **1992**, *13*, 1011−1021.
(17) Marqusee, S.; Robbins, V. H.; Baldwin, R. L. *Proc. Natl. Acad. Sci. U.S.A.* **1989**, *86*, 5286−5290.
(18) Head-Gordon, T.; Stillinger, F. H.; Wright, M. H.; Gay, D. M. *Proc. Natl. Acad. Sci. U.S.A.* **1992**, *89*, 11513−11517.
(19) Blondelle, S. E.; Forood, B.; Houghten, R. A.; Perez-Paya, E. *Biochemistry* **1997**, *36*, 8393−8400.
(20) Levy, Y.; Jortner, J.; Becker, O. M. *Proc. Natl. Acad. Sci. U.S.A.* **2001**, *98*, 2188−2193.
(21) Mortenson, P. N.; Evans, D. A.; Wales, D. J. *J. Chem. Phys.* **2002**, *117*, 1363−1376.
(22) Peng, Y.; Hansmann, U. H. E.; Alves, N. A. *J. Chem. Phys.* **2003**, *118*, 2374−2380.
(23) Zaman, M. H.; Shen, M. Y.; Berry, R. S.; Freed, K. F.; Sosnick, T. R. *J. Mol. Biol.* **2003**, *331*, 693−711.
(24) Kamiya, N.; Watanabe, Y. S.; Ono, S.; Higo, J. *Chem. Phys. Lett.* **2005**, *401*, 312−317.

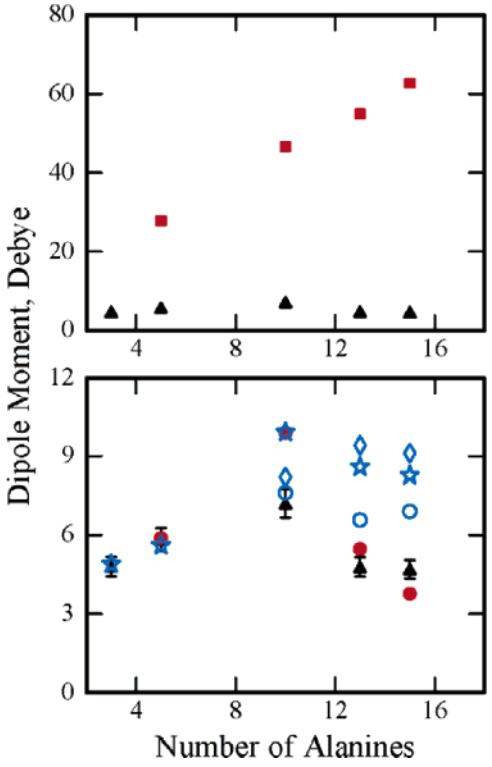

Figure 4. Plots of measured and calculated dipole moments against peptide size at 300 K. The results are plotted on two different scales for clarity. Experimental measurements (filled triangle), energy optimized helices (filled red square), energy optimized β-hairpins (filled red circle), average over the entire free energy map obtained from the Monte Carlo simulations (see text) (blue star), average over the β-sheet region of the free energy map (blue circle), and, average over the globule region of the free energy map (blue diamond).

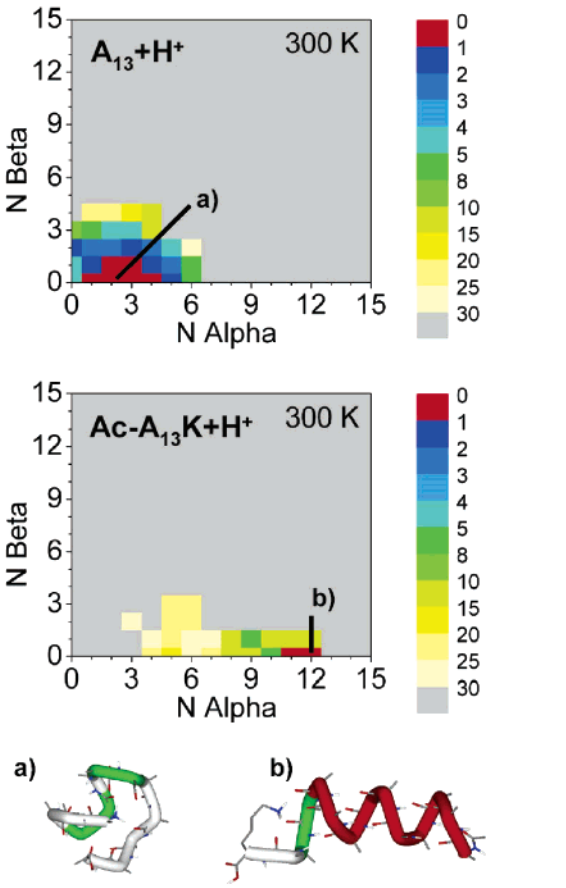

Figure 5. Free energy maps (G/kT) calculated for $A_{13} + H^+$ and Ac-A_{13} $K + H^+$ at 300 K. (a and b) Representative low free energy conformations from the 300 K simulations for $A_{13} + H^+$ and Ac-A_{13} $K + H^+$, respectively.

agreement with the measured values. For $n > 5$ the agreement is less good, although the calculated canonical average dipoles do show a maximum at $n = 10$, in agreement with the measured values. For $n > 5$, secondary structure can emerge, and it is useful to consider average dipole moments for the different secondary structure elements. The total dipole for a peptide is mainly due to the dipoles associated with the peptide bonds (~3.5 D for each one[10]). For α-helices, the dipoles are aligned, and thus the overall dipole for the helix is expected to be large and increase almost linearly with the number of residues (at least within the framework of the simple model employed here). Average dipole moments determined for energy-minimized helices are plotted in the upper half of Figure 4 (as red squares). The measured dipole moments (black triangles) are clearly much smaller than expected for helices. This completely rules out the helical conformation for these peptides.

In an antiparallel β-sheet, the dipoles of the peptide bonds almost cancel, leading to a low dipole moment. The average dipoles determined from the β-sheet regions of the free energy maps (defined for Ac-WA_{13}-NH_2 by the solid box in Figure 2) are plotted in the lower half of Figure 4 (as blue circles). They are slightly larger than the measured values. The average dipoles calculated for the globule region of the free energy maps (blue diamonds) are around 50% larger than for the β-sheet regions (see Figure 1). Thus, for the larger peptides ($n = 13$ and 15) the measured dipoles are in closer agreement with those calculated for β-sheets. Furthermore, the average dipole moments for the globules are expected to systematically increase with peptide size, and thus globules cannot account for the drop in the measured dipole moments for $n > 10$. This drop is a signature of secondary structure formation. Dipole moments calculated for energy-minimized β-hairpin structures (red circles) are in good agreement with the measured dipoles for the larger peptides (see Figure 1).

From the preceding analysis it is evident that the low dipole moments measured for the larger peptides ($n = 13$ and 15) are most consistent with β-sheet conformations. At room temperature, the β-sheets are minima in the free energy maps (see Figure 2), but the globules occupy a larger area, and are more abundant. Thus, it appears that the simulations must underestimate the statistical weights for the β-sheets, either because of inadequate averaging or because the force field overestimates the stability of the globule. However, this is a small discrepancy, and within the expected accuracy limits of the force field.

The measurements that were performed as a function of temperature support the conclusions reached above. The β-sheets should begin to unfold to a random coil conformation as the temperature is raised, and this conformational change should be accompanied by an increase in the dipole moment. It is evident from the results shown in Figure 2 that the dipole moments for Ac-WA_{13}-NH_2 peptide increase significantly between 400 and 500 K. The high temperature values for the dipole moments (see Figure 1) systematically increase as a function of peptide size, a result that is consistent with the Ac-WA_{13}-NH_2 peptide unfolding (or beginning to unfold) to a more random conformation as the temperature is raised.

The conformations of protonated alanine-based peptides have been studied using ion mobility measurements.[25] The presence of a charge, and its position, have a profound effect on the conformation. Protonated Ac-A_nK+H^+ (K = lysine) peptides are helical in the gas phase, while analogues with the lysine at the N-terminus, Ac−KA_n+H^+, adopt a globular conformation. This difference is attributed to the location of the charge. The Ac-A_nK+H^+ peptides are believed to be protonated on the side chain of the C-terminus lysine, and the α-helix is stabilized by an interaction between the charge and the helix macro-dipole (the electrostatic energy is ∼120 kJ mol^{-1}).[10,26] In the Ac−KA_n+H^+ peptides the protonation site is at the N-terminus, which leads to unfavorable interactions with the helix macro-dipole. For A_n+H^+, protonation at the N-terminus amine leads to a globular conformation.[27] Figure 5 shows free energy maps (at 300 K) calculated for $A_{13}+H^+$ (protonated at the N-terminus amine) and Ac-$A_{13}K+H^+$ (protonated at the C-terminus lysine). In agreement with ion mobility measurements, the lowest free energy structures are a globule for $A_{13}+H^+$ and an α-helix for Ac-$A_{13}K+H^+$. In both cases, these structures are also the lowest potential energy structures found in the simulations. Thus, the presence and position of a charge has a profound effect on the conformations of unsolvated alanine-based peptides at room temperature: neutral peptides form β-sheets, peptides protonated near the C-terminus form helices, and peptides protonated near the N-terminus form globules. The formation of an α-helix for peptides protonated near the C-terminal is energy-driven, while the formation of the β-sheet for neutral peptides is entropy-driven.

(25) Hudgins, R. R.; Ratner, M. A.; Jarrold, M. F. *J. Am. Chem. Soc.* **1998**, *120*, 12974−12975.
(26) Sali, D.; Bycroft, M.; Fersht, A. R. *Nature* **1988**, *335*, 740−743.

Conclusions

We have used molecular beam electric deflection measurements in conjunction with parallel tempering Monte Carlo simulations to examine the conformations of neutral alanine-based peptides in the gas phase. At room temperature, unsolvated Ac-WA_n-NH_2 peptides with $n > 10$ have low dipole moments that are consistent with antiparallel β-sheet conformations. These results allow a better understanding of the energetic and entropic effects that govern peptide conformations. At room temperature, the β-sheets are entropically favored for the neutral peptides. Incorporating a charge has a profound effect on the conformation and can cause a switch from a β-sheet to an α-helical or globular structure, depending on its location. Thus the charge, more than anything else, controls the structure.

Acknowledgment. We thank T. Millet, I. Compagnon, and D. Rayane for help in the early experimental part of this work. We gratefully acknowlege the support of the Ministère de la Recherche (ACI jeunes chercheurs) and of the National Institutes of Health.

JA0437499

(27) Hudgins, R. R.; Mao, Y.; Ratner, M. A.; Jarrold, M. F. *Biophys. J.* **1999**, *76*, 1591−1597.